Electronic Supplementary Material (ESI) for Nanoscale.

Supplementary Material for: Effects of Radiation Damage on the Yielding and Fracture of Nanowires

Daniel Vizoso[1] **and Rémi Dingreville**[1,2,*]

[1]Center for Integrated Nanotechnologies, Nanostructure Physics Department, Sandia National Laboratories, Albuquerque, NM 87185, USA
[2]George W. Woodruff School of Mechanical Engineering, Georgia Institute of Technology, Atlanta, GA 30332, USA
[*]rdingre@sandia.gov

ABSTRACT

This supplementary information contains a short summary of the radiation damage insertion and accumulation methodology, an additional figure showing how Young's modulus and yield strain are altered by radiation damage for Au nanowires with diameters of 3, 7, 10, 14, and 20 nm, as well as a short description of 13 videos provided as additional Supplemental Material.

Contents

Supplementary Note 1: Radiation Damage Insertion Approach

All molecular dynamics simulations of the accumulation of radiation damage in Au nanowires were performed using the molecular dynamics code LAMMPS[6,8]. An Embedded Atom Method (EAM) interatomic potential parameterized by Foiles *et al.*[2] was used for all Au molecular dynamics simulations. This interatomic potential was parameterized to reproduce the formation energies of vacancy-type defects, and was also found to match the low-index surface energies and the formation and migration energies of vacancy and self-interstitial defects. This interatomic potential has been used in several other molecular dynamics studies of radiation damage in gold nanostructures[3,5,10]. For all simulations of radiation damage cascades, a short-range repulsive (nuclear stopping) potential was used in conjunction with the EAM potential using the Siegler-Biersack-Littmark[11,12] (ZBL) universal screening function. This ZBL overlay provides a very strong repulsive force when atoms become close together, preventing atoms from getting too close during the ballistic phase of high-energy radiation damage cascades. ZBL switching function parameters of $r_1 = 0.4617$ Å (distance where the ZBL switching function begins) and $r_2 = 1.20$ Å (global cutoff for ZBL interaction)[10] were used, as implemented in the LAMMPS method `pair_style zbl`. Electronic stopping was also included as a frictional drag force following the methods defined in[4,7], with this force being applied to all atoms with kinetic energies greater than 3.79 eV.

Gold nanowire structures were produced by creating cylindrical columns of atom in a face-centered cubic (FCC) phase with a lattice constant of 4.08 Å. Each nanowire had a length equal to twice its diameter, and nanowires with diameters of 3, 7, 10, 14, and 20 nm were created. The longitudinal direction of the nanowires were aligned along the $\langle 001 \rangle$ crystallographic direction, with the boundary along the longitudinal direction being periodic. After the wires were constructed, there were equilibrated at 300 K and zero pressure for a minimum of 50 ps.

Simulations of the accumulation of radiation damage were accomplished via two different methods. For nanowires with diameters of 3 and 7 nm, consecutive cascade simulations were performed. In these simulations, each cascade is initiated by selecting a random atom from the structure as the primary knock-on atom (PKA). The energies of these PKAs were sampled from a primary recoil spectrum computed for a 1 MeV gold ion striking a gold structure. Additional details on the calculation of the primary recoil spectrum can be found in Note 5 of the Supplementary Materials of[9]. After a PKA was selected and provided with the sampled amount of kinetic energy, the system was allowed to evolve under an NVE ensemble for 50 ps, with the surface atoms of the nanowire being held under an overdamped Langevin thermostat at 300 K. Adaptive timestepping was used imediately after the PKA was provided with kinetic energy, such that no atom within the system would move more than 0.02 Åin a single timestep. This timestepping scheme was used for 0.3 ps, after which the system was allowed to evolve with a fixed timestep of 1 fs. For the 3 and 7 nm diameter nanowires, consecutive cascade simulations were run up to a total of 100 cascades.

For nanowires with diameters of 14 and 20 nm, the Reduced Order Atomistic Cascade (ROAC) method[1] was used to simulate the accumulation of radiation damage. In this approach, the collision cascades from a tradiational radiation damage simulation are replaced with a core-shell structure that approximates the displacement cascade by considering the athermal-recombination-corrected displacements-per-atom (arc-dpa) in the shell region, and the replacements-per-atom (rpa) mixing that occurs in the core region. Specific details on how this methodology can be implemented in molecular dynamics simulations can be found in[1,9]. For the ROAC simulations performed for the 14 and 20 nm diameter nanowires, 100 ROAC events were inserted every 70 ps, with the energies of each ROAC event being sampled from the same primary recoil spectrum used for the consecutive cascade simulations. The positions of the ROAC events were randomly distributed throughout the nanowire structures, and ROAC events were only added if they did not include any atoms on the surface of the nanowires, as the ROAC method isn't parameterized to handle cascade-surface interactions. These ROAC simulations were run until the number of displaced atoms equalled the number of atoms in the simulation (i.e., a dose of 1 dpa was reached).

For the 10 nm diameter nanowire, accumulation of radiation damage was accomplished through a hybrid procedure, where the traditional primary knock-on atom (PKA) simulation approach was combined with the reduced-order accelerated cascade (ROAC) approach to accelerate the rate of damage insertion and accumulation up to a final dose of 1 dpa. For these simulations, ROAC events were inserted into the nanowire until a ROAC event was found to overlap with the surface of the nanowire. When this occurred, all of the queued ROAC events would be progressed as normal, then a PKA would be initiated and evolved at the site near the surface. In this way, the interaction of the radiation damage events with the surface was preserved while also accelerating events that occured away from the surface. For a complete description of the hybrid damage insertion technique, additional details regarding the ROAC method, and a complete description of the simulations of radiation damage cascades, the reader is encouraged to examine the Methods section of[9].

Supplementary Note 2: Effect of radiation damage on Young's modulus and yield strain in Au nanowires

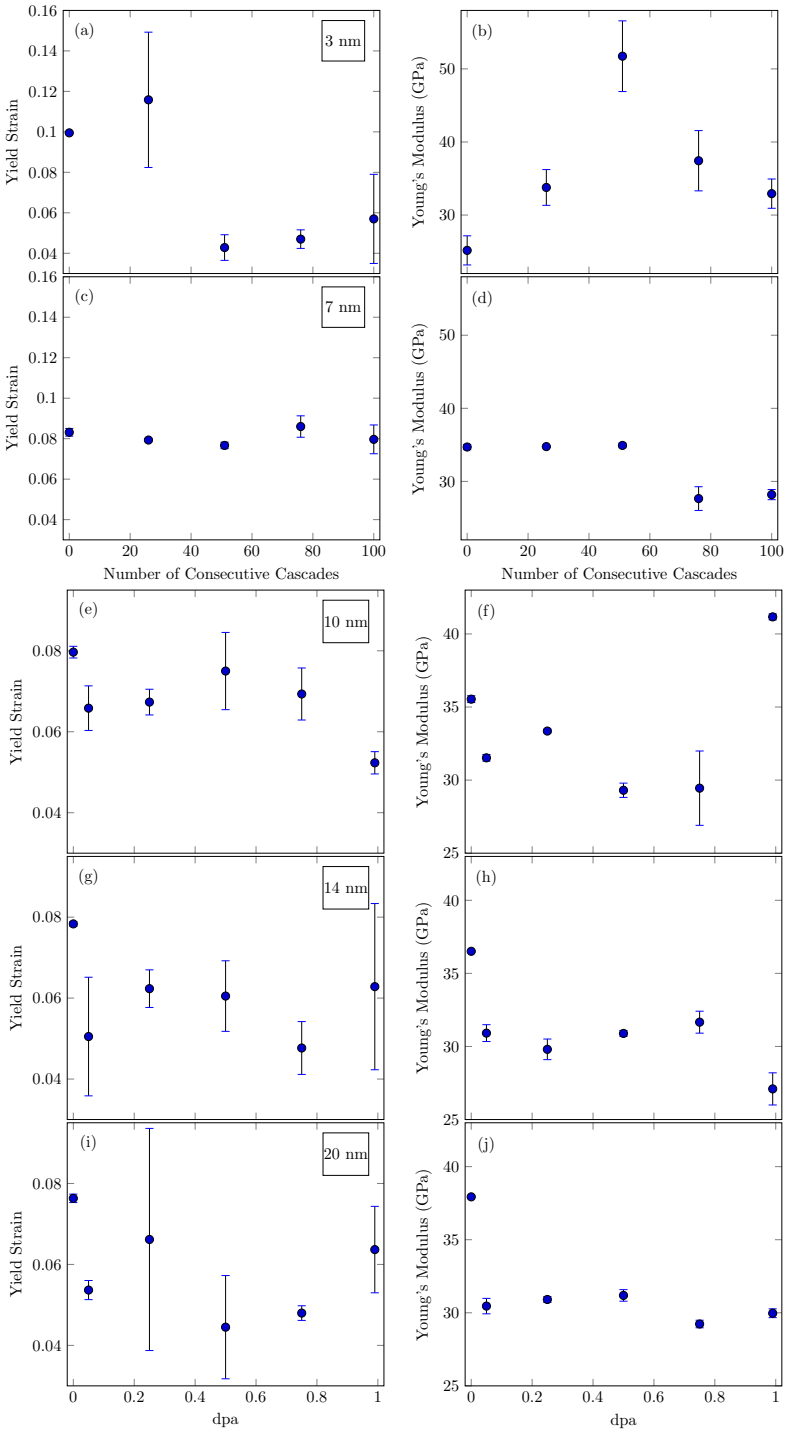

Figure S1. Yield strains and Young's moduli for nanowires at various damage levels, with the corresponding diameter for each row being marked in the top right corner of the yield strain plots.

Supplementary Note 3: Descriptions of Videos of Nanowire Fracture

Videos of molecular dynamics simulations of the tensile fracture of Au nanowires are provided as supplementary materials. Each video contains a description of the initial state of the nanowire at the top of the frame, and an indicator of the applied tensile strain at the bottom of the frame. In these videos, two renderings of each nanowire are shown. The render on the right shows all atoms from the simulation with no structural features highlighted via colors. The render on the left has had half of the disordered surface atoms as well as all FCC atoms removed to show the internal defect structure, with atoms colored according to their structure type as determined by OVITO: red are HCP, white are disordered. The render on the left also shows dislocations, which are colored according to their type as determined by OVITO: green are $\frac{1}{6}\langle 112\rangle$, magenta are $\frac{1}{6}\langle 110\rangle$.

Supplementary videos S1-S5 show the fracture of initially pristine nanowires with diameters of 3, 7, 10, 14, and 20 nm, respectively. Frames from supplementary videos S1 and S3 are included in Fig. 2 (e-h) and (a-d), respectively. Supplementary video S6 shows the fracture of a nanowire with an initial diameter of 3 nm after 50 consecutive cascades. Frames from supplementary video S6 are included in Fig. 6 above panel (a). Supplementary video S7 shows the fracture of a nanowire with an initial diameter of 7 nm after 100 consecutive cascades. Frames from supplementary video S7 are included in Fig. 4 (a) and Fig. 8 (e). Supplementary video S8 shows the fracture of a nanowire with an initial diameter of 10 nm after 0.75 dpa of damage insertion. Frames from supplementary video S8 are included in Fig. 8 (f). Supplementary video S9 shows the fracture of a nanowire with an initial diameter of 10 nm after 0.99 dpa of damage insertion. Frames from supplementary video S9 are included in Fig. 4 (b) and Fig. 7 above panel (b). Supplementary video S10 shows the fracture of a nanowire with an initial diameter of 14 nm after 0.05 dpa of damage insertion. Frames from supplementary video S10 are included in Fig. 8 (g). Supplementary video S11 shows the fracture of a nanowire with an initial diameter of 14 nm after 0.75 dpa of damage insertion. Frames from supplementary video S11 are included in Fig. 6 above panel (b). Supplementary video S12 shows the fracture of a nanowire with an initial diameter of 20 nm after 0.05 dpa of damage insertion. A frame from supplementary video S12 are included in Fig. 4 (c). Supplementary video S13 shows the fracture of a nanowire with an initial diamter of 20 nm after 0.5 dpa of damage insertion. Frames from supplementary video S13 are included in Fig. 8 (h).

Supplementary References

1. E. Chen, C. Deo, and R. Dingreville. Reduced-order atomistic method for simulating radiation damage in metals. *Journal of Condensed Matter Physics*, 32:045402, 2020.
2. S. Foiles, M. Baskes, and M. Daw. Embedded-atom-method functions for the metals Cu, Ag, Au, Ni, Pd, Pt, and their alloys. *Physical Review B*, 37:10378, 1988.
3. E. G. Fu, M. Caro, L. A. Zepeda-Ruiz, Y. Q. Wang, K. Baldwin, E. Bringa, M. Nastasi, and A. Caro. Surface effects on the radiation response of nanoporous Au foams. *Applied Physics Letters*, 101:191607, 2012.
4. C.-W. Lee, J. A. Stewart, R. Dingreville, S. M. Foiles, and A. Schleife. Multiscale simulations of electron and ion dynamics in self-irradiated silicon. *Physical Review B*, 102:024107, 2020.
5. W. Liu, P. Chen, R. Qiu, M. Khan, J. Liu, M. Hou, and J. Duan. A molecular dynamics simulation study of irradiation induced defects in gold nanowire. *Nuclear Instruments and Methods in Physics Research Section B: Beam Interactions with Materials and Atoms*, 405:22–30, 2017.
6. S. Plimpton. Fast parallel algorithms for short-range molecular dynamics. *Journal of Computational Physics*, 117:1–19, 1995.
7. J. A. Stewart, G. Brookman, P. Price, M. Franco, W. Ji, K. Hattar, and R. Dingreville. Characterizing single isolated radiation-damage events from molecular dynamics via virtual diffraction methods. *Journal of Applied Physics*, 123:165902, 2018.
8. A. P. Thompson, H. M. Aktulga, R. Berger, D. S. Bolintineanu, W. M. Brown, P. S. Crozier, P. J. in't Veld, A. Kohlmeyer, S. G. Moore, T. D. Nguyen, R. Shan, M. J. Stevens, J. Tranchida, C. Trott, and S. J. Plimpton. LAMMPS - a flexible simulation tool for particle-based materials modelling at the atomic, meso, and continuum scales. *Computer Physics Communications*, 271:108171, 2022.
9. D. Vizoso, M. Kosmidou, T. J. Balk, K. Hattar, C. Deo, and R. Dingreville. Size-dependent radiation damage mechanisms in nanowires and nanoporous structures. *Acta Materialia*, 215:117018, 2021.
10. C. G. Zhang, Y. G. Li, W. H. Zhou, L. Hu, and Z. Zeng. Anti-radiation mechanisms in nanoporous gold studied via molecular dynamics simulations. *Journal of Nuclear Materials*, 466:328–333, 2015.
11. J.F. Ziegler, J.P. Biersack, and U. Littmark. *The Stopping and Range of Ions in Matter, Vol. 1.* Pergamon, New York, 1985.

12. J.F. Ziegler, M.D. Ziegler, and J.P. Biersack. SRIM–the stopping and range of ions in matter (2010). *Nucl. Instrum. Methods Phys. Res. B*, 268(11-12):1818–1823, 2010.